

Synergy of Nano Silica and Anionic Surfactant Fluid as Chemical Enhanced Oil Recovery

Khasan Rowi¹, Agus Subagio¹, Ngadiwiyana¹, Heydar Ruffa Taufiq¹, Muhammad Mufti Azis², Bayu Dedi Prasetyo³, Victor Sitompul⁴, Sumadi Paryoto⁴, Denie Tirta Winata⁴, Tino Diharja⁴, Michael Arya Yutaka⁴, Abimanyu Putra Syarifudin⁴, Wahyu Firmansyah⁴, and Harry Koestono⁴

¹Nano Technology Laboratory, Integrated Laboratory. Diponegoro University
Prof. Soedarto, SH street, Semarang 50275, Indonesia.

²Department of Chemical Engineering, Faculty of Engineering, Gadjah Mada University
Sleman Street, Special Region of Yogyakarta 55281, Indonesia.

³BBPMGB LEMIGAS
Ciledug Raya Kavling street No 109, Jakarta 12230, Indonesia.

⁴Technology Development 1, PT Pertamina (Persero)
Sope Del Tower Lantai 50, Mega Kuningan Barat III street, Jakarta Selatan 12950, Indonesia.

Corresponding Author: Khasan Rowi (khasanrowi@students.undip.ac.id)

Manuscript received: October 21th, 2025; Revised: November 14th, 2025

Approved: December 09th, 2025; Available online: December 18th, 2025; Published: December 19th, 2025.

ABSTRACT - Silica nanofluids attract significant attention for enhanced oil recovery (EOR) applications due to their ability to alter rock wettability. However, silica nanofluids exhibit limitations in thermal stability. The addition of anionic surfactants aims to overcome these limitations. The synergistic anionic surfactants are added to address the thermal stability issues of silica nanofluids. The synergy interaction between silica nanoparticles (SNPs) and anionic surfactants enhances wettability alteration, reduces interfacial tension (IFT), improves thermal stability, and increasing oil recovery. This study investigates the synergistic effects of SNPs, alpha olefin sulfonate (AOS) surfactant, and disodium laureth sulfosuccinate (DLS) co-surfactant in nanofluid formulations applied to sandstone reservoirs. Laboratory experiments employ colloidal nano silica with two particle sizes, 8 nm (SNP-01) and 3 nm (SNP-02), combined with AOS-DLS anionic surfactants at various concentrations. The study showed that the silica nanofluid remains stable for up to 3 months at temperatures below 80°C for both SNP types at a concentration of 0.1% with surfactant concentrations 0.3% AOS and 0.3% DLS in 3% brine solution. The addition of SNPs decreases the contact angle, whereas surfactants do not significantly affect the contact angle; however, surfactant effectively reduce the IFT, while nano silica shows minimal influence on IFT values. Core flooding analysis showed that the SNP-02 nanofluid produced the highest recovery factor of 12.1% OOIP. Furthermore, SEM analysis showed that silica nanofluid injection removes surfactant impurities and enhances rock porosity.

Keywords: silica nano fluid, EOR, thermal stability, core flooding, wettability.

Copyright © 2025 by Authors, Published by LEMIGAS

How to cite this article:

Khasan Rowi, Agus Subagio, Ngadiwiyana, Heydar Ruffa Taufiq, Muhammad Mufti Azis, Bayu Dedi Prasetyo, Victor Sitompul, Sumadi Paryoto, Denie Tirta Winata, Tino Diharja, Michael Arya Yutaka, Abimanyu Putra Syarifudin, Wahyu Firmansyah, and Harry Koestono, 2025, Synergy of Nano Silica and Anionic Surfactant Fluid as Chemical Enhanced Oil Recovery, Scientific Contributions Oil and Gas, 48 (4) pp. 337-355. DOI org/10.29017/scog.v48i4.1951.

INTRODUCTION

Crude oil remains a major source of the world's energy supply. However, the petroleum industry faces challenges, including the depletion of new conventional oil reserves and declining production from existing reservoirs. Typically, only about one-third of the oil in conventional reservoirs is recovered through primary and secondary oil recovery techniques. The remaining oil-in-place becomes the focus of EOR processes. EOR, also known as tertiary recovery, enhances extraction by improving recovery rates. Current EOR methods can recover 30% to over 60% of the hydrocarbons, compared with 20% to 40% achieved with primary and secondary recovery methods (Malozyomov et al., 2023).

Chemical enhanced oil recovery (CEOR) is considered the most promising method due to its high efficiency and technical and economic feasibility. The chemicals typically used for injection include alkali, surfactants, and polymers.

Despite its potential, chemical EOR has several drawbacks, including the need for large amounts of chemicals, high cost, and the potential for chemical degradation in the reservoir. In addition, environmental concerns, particularly the potential for groundwater contamination, pose significant challenges to the broader application of this method (Alsaba et al. 2020; Bratovcic 2023; Franco et al., 2021).

In recent years, nanotechnology has attracted increasing interest in the oil and gas industries. Numerous studies have provided comprehensive reviews on the potential applications of nanotechnology in this sector (Al-Shargabi et al., 2022; Davoodi 2022; Panchal 2021). Among

various types of nanoparticles, silica nanoparticles (SNPs) have been extensively researched for EOR applications (Hadia et al. 2021). Nanoparticles can be integrated with different chemical enhanced oil recovery (EOR) methods to improve oil recovery efficiency (Fathaddin et al., 2025). Pramana et al. (2023) (DN & Szafdarian, 2023) investigated the foam stability of AOS during CO₂ injection in the presence of silica nanoparticles (SNPs), demonstrating a 10.23% increase in foam half-life. Meanwhile, Paramastya et al. (2019) (Paramastya et al. 2019) conducted a Huff and Puff evaluation using silica nanoparticles combined with surfactants (nanosurfactants) in a marginal oil field in South Sumatra, Indonesia. Their results indicated that the application of nanosurfactants significantly improved EOR performance and provided greater economic benefits.

In EOR, these nanoparticles are primarily utilized as nanofluids. A nanofluid is defined as a base fluid containing nanoparticles with an average particle size of less than 100 nm in colloidal suspension (Philip 2023). Typically, nanofluids made by adding various nanoparticles to water or brine are used to enhance water flooding recovery. The EOR mechanisms of nanofluids have been explored in the literature, which mainly include disjoining pressure, pore channel plugging, increased viscosity of injection fluids, reduction of IFT, wettability alteration, and prevention of asphaltene precipitation (Bila 2021; Sharma et al. 2024; Sircar et al. 2022). For EOR to be successful, maintaining the long-term colloidal stability of nanoparticles under harsh reservoir conditions is critical. Nanoparticle dispersions are prone to losing colloidal stability in high salinity and high-temperature environments, leading to agglomeration (Hu et al.,

2023). Agglomeration presents a significant challenge in the preparation of nanofluids, as instability can negate their potential benefits when injected into reservoirs. The use of nanoparticle fluids combined with surfactants in CEOR has garnered significant interest among researchers. This surfactant nanofluid, which consists of both nanoparticles and surfactants, can enhance stability and improve microscopic displacement efficiency through mechanisms such as IFT reduction, wettability alteration, and decreased adsorption during transport through porous media (Dordzie & Dejam 2021; Fu et al., 2022; Mmbuji et al. 2023).

Recently, (3- lycidyloxypropyl) trimethoxysilane (GLYMO) has been proposed by many researchers as a stabilizer for silica nanodispersions under harsh conditions. (Hadia et al., 2021) reported the synthesis of silica nanofluids with high thermal stability under high temperature and high salinity conditions using a surface modification process involving 3-(Dimethyl (3-(Trimethoxysilyl) Propyl) Ammonio) Propane-1-Sulfonate (SBS) and surfactant GLYMO. The results of Turbiscan analysis indicated that the silica nanofluid could remain stable for up to 6 months at 60 °C and 3.5% NaCl salinity. However, the reported methods and procedures for stabilizing SNPs are complex, often requiring high temperature, multiple steps, and initial grafting with chemical linkers. As a result, these processes tend to be costly and energy-intensive. Therefore, there is significant interest in developing more cost- effective surface treatment and grafting strategies that can be integrated with conventional EOR technologies.

To maximize oil recovery during nanofluid flooding, it is essential to understand the parameters that influence the displacement process. Factors such as temperature, type of base fluid, nanoparticle (NP) characteristics, NP size, and injection time play significant roles in the performance of silica nanofluid flooding (Shayan Nasr et al. 2021).

Furthermore, the choice of raw material for silica nanoparticles is crucial for producing stable silica nanofluids. Two primary techniques are commonly used for nanofluid synthesis. The first is

the two-step technique, where dry nanoparticle powders are synthesized and then dispersed into a base fluid. However, due to nanoparticles' high surface energy, aggregation and clustering frequently occur, necessitating additional treatments, such as high-shear homogenization

and ultrasonication, to mitigate them. Alternatively, the one-step technique combines nanoparticle synthesis and nanofluid preparation in a single process. This approach eliminates the need for drying, storage, transportation, and subsequent dispersion of nanoparticles, thereby reducing the likelihood of aggregation and enhancing nanofluid stability (Li et al. 2020).

This study addresses the lack of a systematic evaluation of silica nanoparticle size in combination with anionic surfactants to improve the thermal stability and EOR performance of silica nanofluids. We investigated how the colloidal silica nanoparticles' diameter and the addition of the anionic surfactant AOS and co- surfactant DLS influence nanofluid thermal stability using a one-step synthesis method, which remains underexplored compared to traditional two-step routes. Furthermore, this research provides the first evaluation of silica nanofluid performance in crude oil from Sumatra sandstone reservoirs, aiming to develop a cost- effective, readily producible nanofluid tailored for field-scale EOR applications.

METHODOLOGY

Material

The experiment utilized two types of colloidal silica nanoparticles: SNP-01 (8 nm) and SNP-02 (3 nm), synthesized by sol-gel from sodium silicate raw materials (Table 1), sourced from the nanotechnology laboratory at Diponegoro University. Commercial anionic surfactants, specifically alpha olefin sulfonate (AOS) 40% v/v with specification yellow color, specific gravities of 0.97 g/ml, pH 8.0 from Rachara Chemical Technology, and disodium laureth sulfosuccinate (DLS) 32.28% v/v with specification clear appearance, pH 6.0-7 from Evonik, were used. The light crude oil was obtained from the reservoir Jambi field, Sumatera at PT. Pertamina,

characterized by an API gravity of 49.80, a kinematic viscosity of 0.6323 cSt, and a reservoir temperature range of 60-70 °C (Table 2). Core samples used were upper gray Berea with 20% porosity and permeability ranging from 266 to 359 mD, and synthetic brine containing pharmaceutical-grade NaCl and distilled water.

Methods

Nanofluid preparation

Nanofluids were prepared according to predetermined parameters across varying surfactant concentrations, salinity levels, and silica nanoparticle diameters. The silica nanofluids were created by mixing silica nanoparticles at a concentration of 0.1 wt.% v/v with brine NaCl at 1%, 2%, and 3% w/v, then adding anionic surfactants (AOS-DLS) at various concentrations: 0%:0%, 0%:0.3%, 0.1%:0.3%, 0.2%:0.3%, and 0.3%:0.3% w/v. The resulting mixture was stirred electronically at 500 rpm and 60 °C for 30 minutes, followed by ultrasonication at 20 kHz for 5 minutes.

Characterization of silica nanofluid

Thermal stability

Thermal stability tests of the nanodispersions were conducted through visual observations. Samples were placed in glass tubes, tested, and stored in ovens at 60 °C, 80 °C, and 100 °C for 3 months. Daily observations were made to assess the stability of the silica nanofluids. The samples tested included those without surfactant additions across different salinity levels, and those with surfactants at various concentrations.

Transmission electron microscopy (TEM)

This test aims to assess the influence of brine and surfactants on the diameter of silica nanoparticles in nanofluid formulations. Testing was carried out on nanofluid samples without drying. Ideally, the resulting diameter of the silica nanoparticles from the nanofluid formulation should not differ significantly from that of pure silica nanoparticles. The optimal sample from this testing will be utilized for core flooding experiments.

Table 1. Data analysis of silica nanoparticles, laboratory Nanotechnology, Diponegoro University

| Properties | SNP-01 | SNP-02 |
|------------------------------|-------------------|------------------|
| Color | Colloidal white | Clear |
| Diameter size (nm) | 8 | 3 |
| Aggregate diameter (nm) | 2,756 | 86 |
| Particle shape | Spherical | Spherical |
| Concentration (%) | 12.7 | 0.25 |
| pH | 8.69 | 8.1 |
| Functional group | Si-OH and Si-O | Si-OH and Si-O |
| Stability (room temperature) | Short-term stable | Long-term stable |

Table 2. Data analysis of crude oil reservoir Jambi field, from Sumatra, Indonesia

| Determination | Unit | Result | Method |
|------------------|-------|---------|----------------------|
| Density at 15 °C | g/cm2 | 0.76 | ASTM D.5002 |
| °API Gravity | - | 49.80 | ASTM D.5002 |
| Kin. Viscosity | cSt | 0.6323 | Ostwald |
| Pour Point | oC | -33 | ASTM D.97 |
| Asphaltene | %wt | 0.018 | IP.143 |
| Wax content | %wt | 0.07263 | IFP-Alk.Eter |
| Saturated | %wt | 15.43 | Chromotogtafi column |

Interface tension (IFT)

Interfacial tension (IFT) testing was conducted using a spinning drop interfacial tensiometer (TX-500D). The IFT value was measured using the Young-Laplace equation, which requires evaluating the droplet's curvature. Measurements were taken at 60 °C, 3000 rpm, and 1 atm.

Contact angle (wettability)

Contact angle testing employed a captive-drop method, using a camera connected to a computer or laptop to capture images of oil droplets at the tip of a needle in contact with the core slice, which was adhered to a transparent glass surface. Thin sections were prepared by cutting small slices from a clean core plug. These thin sections were then immersed in a silica nanofluid solution using a sessile drop apparatus at 60 °C for 1 hour. Subsequently, crude oil was injected from beneath the thin section to measure and analyze the contact angle between the crude oil and the core surface.

Injectivity

An injectivity test was performed on the silica nanofluids to evaluate the potential for pore plugging in reservoir rock. The test utilized SNP01 and SNP02 nanofluid solutions, each containing 0.3% AOS and 0.3% DLS surfactants. The injection was conducted at a flow rate of 0.3-0.8 cc/minute, at a temperature of 60 °C, using an upper gray Berea sandstone core. The injectivity test scenario consisted of three stages: a pre-flush with brine, a chemical flood with a silica nanofluid, and a post-flush with brine.

Core flooding

The upper gray Berea core, measuring 3.1 inches in length and 1.5 inches in diameter, was first analyzed for its porosity and permeability. Subsequently, the core was cleaned and saturated with brine by immersing it in brine, then placed in a vacuum oven to ensure complete saturation. The core was saturated with brine for 5 hours before being put into the core holder. It was then further saturated with crude oil and left (aged) for 48 hours at 60 °C. The aged, saturated core was inserted into the core holder of the core flooding apparatus. The flooding sequence consisted of sequential injections of 3% NaCl brine, silica nanoflooding, and a post-flush using formation water. The entire core flooding process was conducted at 60 °C with an injection rate of 0.3 cc/minute.

Scanning electron microscope (SEM)

SEM analysis allows detailed observation of the surface of a material or object, including its topography and the rock structure used in core flooding. The analyzed samples include rock cores before and after core flooding, enabling evaluation of pore structure conditions. This analysis was carried out by cutting a section from the center of the core sample.

RESULT AND DISCUSSION

The synthesis of silica nanofluids was conducted with two treatment variations: one without the addition of surfactants and the other with surfactants. The silica nanofluid was



Figure 1. Synthesis process of nanofluid

formulated by dissolving SNPs in a salt solution at various concentrations without heating. The research on nanofluid synthesis without surfactants (Figure 2) focused on assessing the stability characteristics of pure silica nanoparticles at multiple salt concentrations and reservoir temperatures, immediately after preparation. This approach aimed to identify their potential use as silica nanofluids in specific reservoirs with conditions that align with the findings of this study. Based on the observations, it was found that SNP-01 and SNP-02 silica nanoparticles were visually well dispersed at various NaCl concentrations.

Conversely, the research on the synthesis of nanofluids with surfactants (Figure 3) aimed to evaluate the effects of combining silica nanoparticles with surfactants in a 3% NaCl solution, based on the nanofluid properties observed immediately after preparation. Visual observations revealed that the SNP-01 nanofluid with 0.0% AOS and 0.0% DLS concentrations appeared more turbid (Figure 2a). This turbidity may have resulted from nanoparticle aggregation during heating of the saline solution. In contrast, nanofluids formulated with other surfactants could help minimize silica nanoparticle agglomeration. However, different results were observed in the SNP-02 nanofluid (Figure 2b). The SNP-02 nanofluid without surfactants (0.0% AOS and 0.0% DLS) appeared more evident than those containing AOS:DLS combinations of 0%:0,3%, 0,1%:0,3%, 0,2%:0,3%, and 0,3%:0,3%. Interestingly, the clarity of the nanofluids increased with higher surfactant concentrations. The exact reason for this phenomenon is still unknown. Additionally, pH measurements showed that the average pH of the nanofluids was approximately 8. This investigation aimed to enhance the overall performance and stability of nanofluids for potential EOR applications.

Characteristics of silica nanofluid

The thermal stability test results for nanofluids without surfactants using SNP 01 silica nanoparticles indicated that the nanofluids were unstable, as evidenced by the formation of the white deposits at the bottom of the fluid. Precipitation was observed on the first day across

all salinity and test temperature conditions. Detailed observations are presented in Table 3.

Table 3. Thermal stability of nanofluids without surfactants in SNP 01

| Nano Silica Type | Brine (%) | SNPs (%) | Temperature (°C) | Stability |
|------------------|-----------|----------|------------------|-----------|
| SNP-01 | 1 | 0.1 | 60 | Unstable |
| | 2 | 0.1 | 60 | Unstable |
| | 3 | 0.1 | 60 | Unstable |
| | 1 | 0.1 | 80 | Unstable |
| | 2 | 0.1 | 80 | Unstable |
| | 3 | 0.1 | 80 | Unstable |
| | 1 | 0.1 | 100 | Unstable |
| | 2 | 0.1 | 100 | Unstable |
| | 3 | 0.1 | 100 | Unstable |

Table 4. Thermal stability of nanofluids without surfactants in SNP 02

| Nano Silica Type | Brine (%) | SNP (%) | Temperature (°C) | Stability |
|------------------|-----------|---------|------------------|-----------|
| SNP-02 | 1 | 0.1 | 60 | Unstable |
| | 2 | 0.1 | 60 | Unstable |
| | 3 | 0.1 | 60 | Unstable |
| | 1 | 0.1 | 80 | Unstable |
| | 2 | 0.1 | 80 | Unstable |
| | 3 | 0.1 | 80 | Unstable |
| | 1 | 0.1 | 100 | Unstable |
| | 2 | 0.1 | 100 | Unstable |
| | 3 | 0.1 | 100 | Unstable |

The visual observations of the thermal stability of nanofluids without surfactants using SNP 02 revealed that these nanofluids remained stable for the first month at salt concentrations ranging from 1-3% and temperatures of 60 °C and 80 °C. However, at 100 °C, the nanofluids began to settle within the first week. Notably, the variation in salt concentration did not significantly affect the stability of the nanofluids across the different temperatures tested, as detailed in Table 4.

The findings indicate that nanofluids utilizing SNP 02 demonstrate a good level of stability across various salt concentrations and temperature conditions. In contrast, nanofluids with SNP 01 exhibit a low level of stability under similar variations in temperature and salinity. Additionally, visual observations of the thermal stability of nanofluids with surfactants using SNP 01 showed

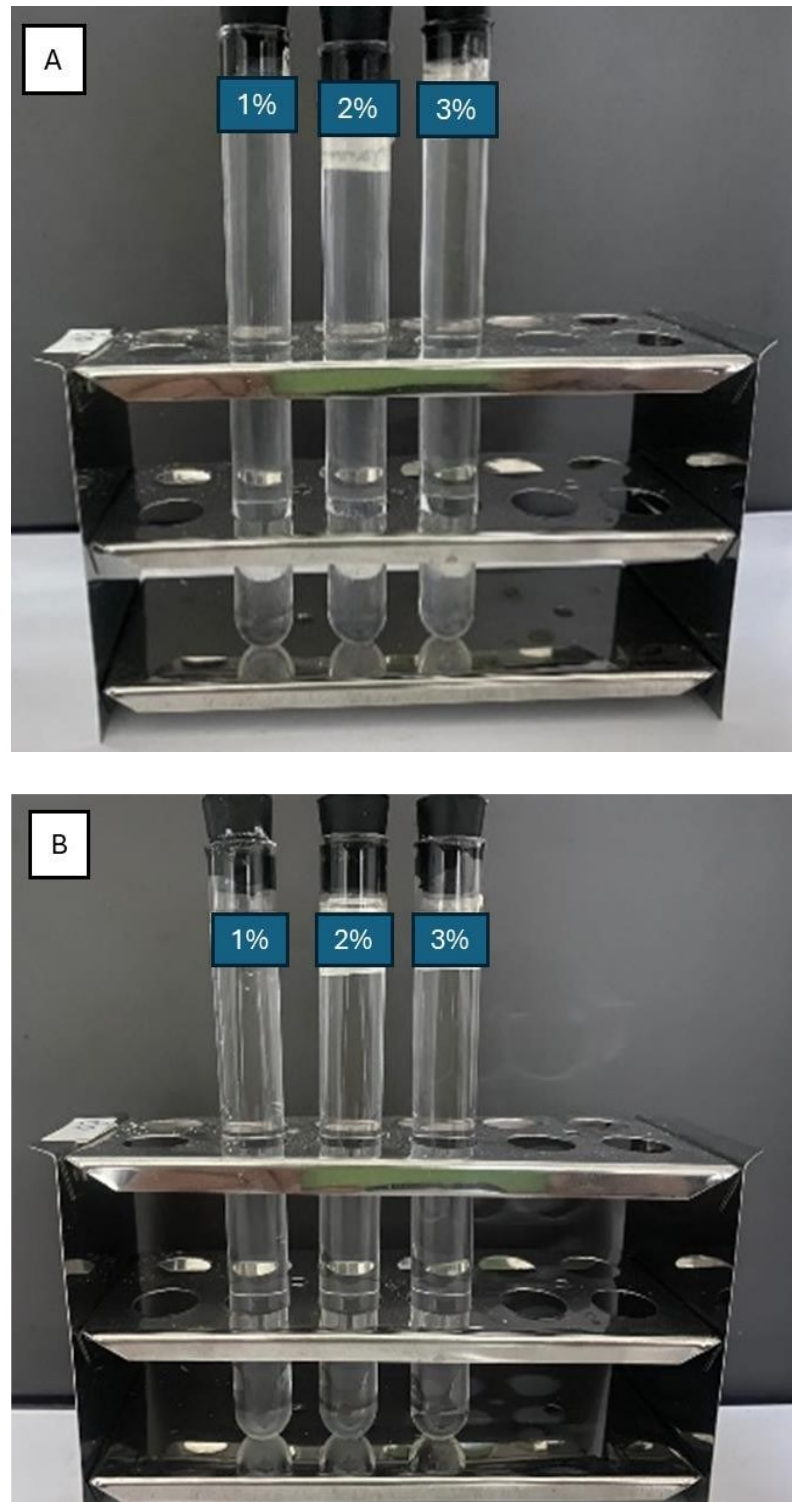


Figure 2. Results of silica nanofluid without surfactants; a) SNP-01, from the left NaCl 1%, 2% and 3%, b) SNP 02, from the left NaCl 1%, 2% and 3%.

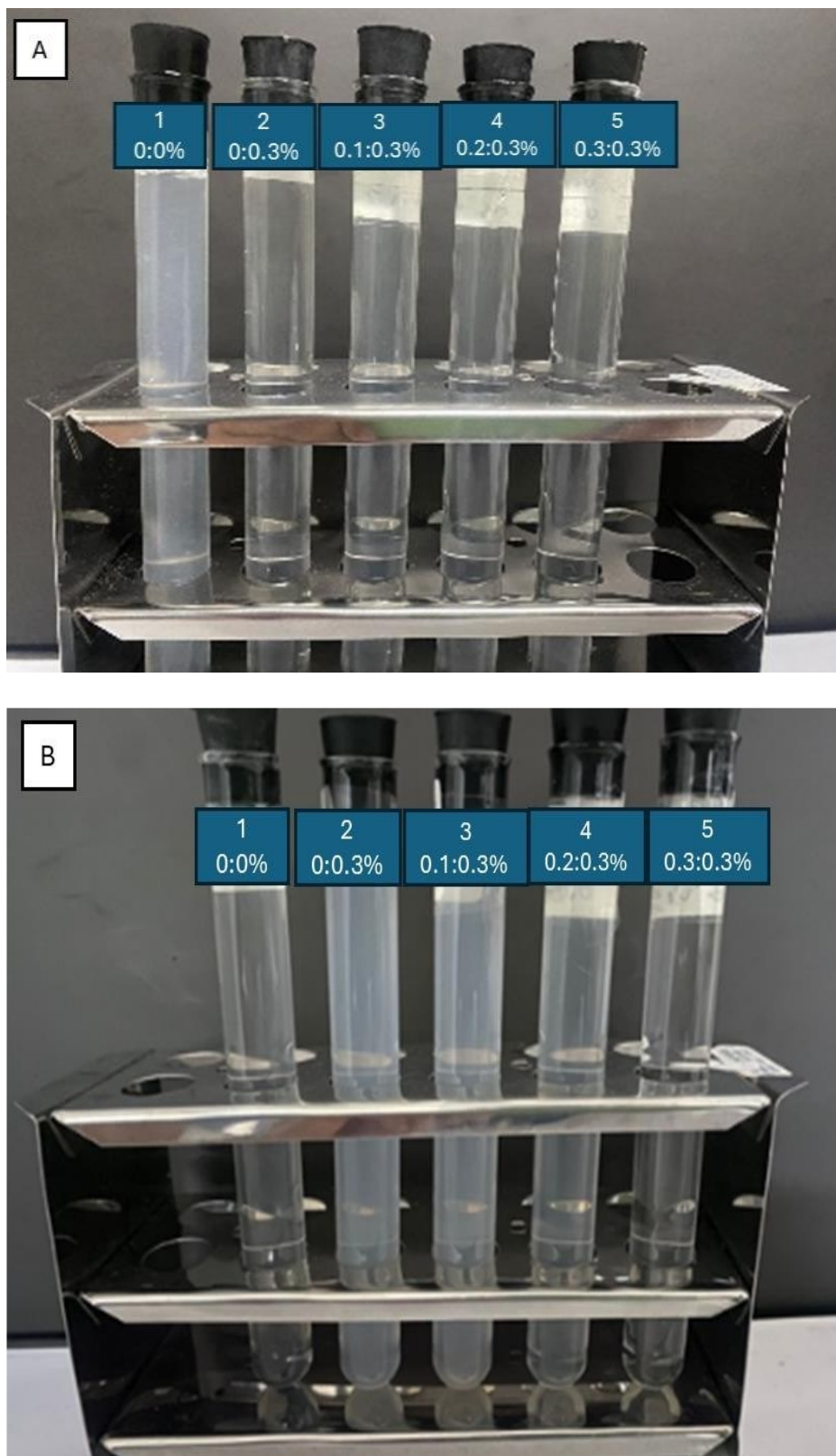


Figure 3. Results of nanofluid with surfactants; a) nano silica SNP 01 with surfactant AOS:DLS, b) nano silica SNP 02 with surfactant AOS:DLS - variation in AOS:DLS concentration; from the left 1) 0%:0%, 2) 0%:0,3%, 3) 0,1%:0,3%, 4) 0,2%:0,3%, 5) 0,3%:0,3%.

that nanofluids containing DLS and AOS at concentrations of 0.3% each remained stable at temperatures of 60 °C and 80 °C for 12 weeks (3 months), as illustrated in Table 5. However, at 100 °C, precipitates formed on the first day across all surfactant concentration variations. For nanofluids incorporating SNP 02, similar results were observed; the nanofluids with surfactant concentrations of DLS 0.3% and AOS 0.3% also maintained stability at 60 °C and 80 °C for 12 weeks (3 months), consistent with the observations for SNP 01 (Table 6). A comparison of the results in Table 3 and 4 with those in Table 5 and 6 indicates

that the addition of the AOS surfactant and DLS co-surfactant, each at a concentration of 0.3%, significantly enhances the thermal stability of silica nanofluids. This formulation remained stable for up to 3 months at temperatures below 80 °C. Additional studies are required to evaluate the effectiveness of these formulations for stability periods exceeding three months. Furthermore, the adsorption of surfactants onto the nanoparticles (NPs) surfaces plays a crucial role in preventing aggregation in nanofluids. The surfactants form a protective layer around the NPs, consisting of long

Table 5. Thermal stability of nanofluids with surfactants - SNP 01

| Nano silica | Temperature (°C) | Anionic Surfactant (%) | | Result |
|-------------|------------------|------------------------|-----|----------|
| | | AOS | DLS | |
| SNP-01 | 60 | 0 | 0 | Unstable |
| | | 0 | 0.3 | Unstable |
| | | 0.1 | 0.3 | Unstable |
| | | 0.2 | 0.3 | Unstable |
| | | 0.3 | 0.3 | Stable |
| | | 0 | 0 | Unstable |
| | 80 | 0 | 0.3 | Unstable |
| | | 0.1 | 0.3 | Unstable |
| | | 0.2 | 0.3 | Unstable |
| | | 0.3 | 0.3 | Stable |
| | | 0 | 0 | Unstable |
| | | 0 | 0.3 | Unstable |
| 100 | 60 | 0.1 | 0.3 | Unstable |
| | | 0.2 | 0.3 | Unstable |
| | | 0.3 | 0.3 | Unstable |
| | 80 | 0 | 0 | Unstable |
| | | 0 | 0.3 | Unstable |
| | | 0.1 | 0.3 | Unstable |

Table 6. Thermal stability of nanofluids with surfactants - SNP 02

| Nano silica | Temperature (°C) | Anionic Surfactant (%) | | Result |
|-------------|------------------|------------------------|-----|----------|
| | | AOS | DLS | |
| SNP-01 | 60 | 0 | 0 | Unstable |
| | | 0 | 0.3 | Unstable |
| | | 0.1 | 0.3 | Unstable |
| | | 0.2 | 0.3 | Unstable |
| | | 0.3 | 0.3 | Stable |
| | | 0 | 0 | Unstable |
| | 80 | 0 | 0.3 | Unstable |
| | | 0.1 | 0.3 | Unstable |
| | | 0.2 | 0.3 | Unstable |
| | | 0.3 | 0.3 | Stable |
| | | 0 | 0 | Unstable |
| | | 0 | 0.3 | Unstable |
| 100 | 60 | 0 | 0 | Unstable |
| | | 0 | 0.3 | Unstable |
| | | 0.1 | 0.3 | Unstable |
| | 80 | 0 | 0 | Unstable |
| | | 0 | 0.3 | Unstable |
| | | 0.1 | 0.3 | Unstable |

loops and tails extending into the surrounding fluid. This steric stabilization mechanism effectively maintains nanoparticle dispersion, allowing the nanofluids to remain stable over extended periods (Behera et al. 2024).

Microstructure of silica nanofluid

The analysis of silica nanofluids containing surfactant AOS 0.3%-DLS 0.3% using Transmission Electron Microscopy (TEM) (Figure 4) indicates that interactions between silica nanoparticles and surfactants lead to the formation of aggregates with varying shapes and sizes. Figures 3a and 3c show that nanofluids without surfactants exhibit a uniform particle distribution, predominantly spherical morphology, and brighter contrast. In contrast, Figures 3b and 3d demonstrate that the addition of surfactants alters the particle distribution, as indicated by darker contrast and more irregular particle shapes. Despite the formation of aggregates, these structures appear to be mobile, suggesting adaptability within the pore spaces and a reduced likelihood of pore clogging. This interpretation is further supported by injectivity and core flooding results, which confirm efficient fluid transport through the rock matrix.

Wettability silica nanofluid

The contact angle measurements were conducted under fixed parameters, including room temperature, a 3% NaCl salt concentration, Jambi field crude oil from Sumatra, synthetic upper gray Berea sandstone, and a nano-silica concentration of 0.1%, along with AOS and DLS surfactant concentrations of 0.3% each. The variable parameters included the types of fluids (salt solutions, surfactant solutions, nano-silica solutions, and nanofluid solutions) and the types of nano-silica (SNP 01 and SNP 02). The results indicated that the addition of nano-silica significantly lowered the contact angle. In the NaCl solution, the contact angle measured 60.84°. With the addition of surfactants, this decreased slightly to 58.75°. However, introducing nano-silica into the salt solution resulted in a more substantial reduction, with contact angles of 40.96° for SNP 01 and 37.33° for SNP 02. The best results were achieved when combining nano-silica and surfactant in the salt solution, yielding contact

angles of 36.63° for SNP 01 and 27.68° for SNP 02. Thus, the synergy of SNP 02 with the AOS-DLS surfactant was found to be the most effective in reducing the contact angle. The analysis data is illustrated in Figure 5. Figure 5. Effect of fluid solution type on contact angle, illustrating the reduction of contact angle on sandstone surfaces due to silica nanofluid treatment and its interaction with anionic surfactants. The results of this study align with the findings of (Ahmed et al. 2020), who measured the contact angles of pure silica nanofluids and those combined with two different brands of olefin sulfonate surfactants. Ahmed's results indicate that the addition of surfactants to silica nanofluids contributes to a reduction in the contact angle. The observed changes in wettability on the sandstone surface can be attributed to the synergistic effects of the opposing charges of the nanoparticles and the presence of surfactants in the nanofluid (Kumar et al. 2022).

Interfacial tension (IFT) silica nanofluid

The analysis reveals that IFT value of nanofluids using SNP 01 dropped sharply to approximately 0.04 mN/m upon the addition of 0.3 wt.% DLS (co-surfactant). Subsequent additions of AOS at 0.1, 0.2, and 0.3 wt.% did not result in any further meaningful IFT reduction. The best value IFT was achieved in nanofluids with DLS and AOS surfactants at concentrations of 0.3%-0.3% each, resulting in an IFT of 3.7×10^{-2} mN/m (Figure 6). Value IFT nanofluida 3.7×10^{-2} mN/m is within the range ultra-low IFT (in the range 10^{-2} to 10^{-3} mN/m) (Dong et al., 2018). The observed decrease in IFT value can be attributed to the presence of surfactants, which effectively lower the surface tension. This reduction is beneficial for decreasing IFT values and enhancing the emulsification of oil in water. Surfactants facilitate the formation of microemulsions, allowing oil hydrocarbons to dissolve in water or vice versa. Consequently, surfactants play a crucial role in reducing the IFT value of nanofluids, thereby improving their performance in EOR applications. In general, IFT reduction is a critical parameter in chemical flooding processes (Abraham et al., 2020). The combination of AOS-DLS surfactant with

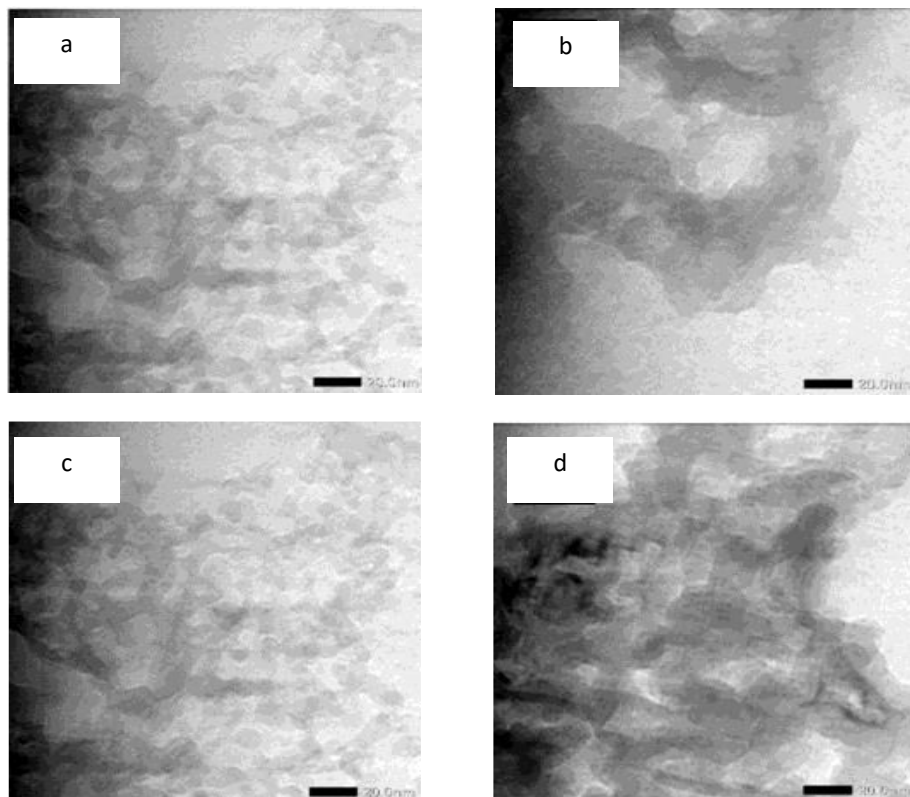


Figure 4. Results of TEM analysis; a) nanofluids without surfactants SNP 01, b) nanofluids with surfactants SNP 01, c) nanofluids without surfactants SNP 02, d) nanofluids with surfactants SNP 02.

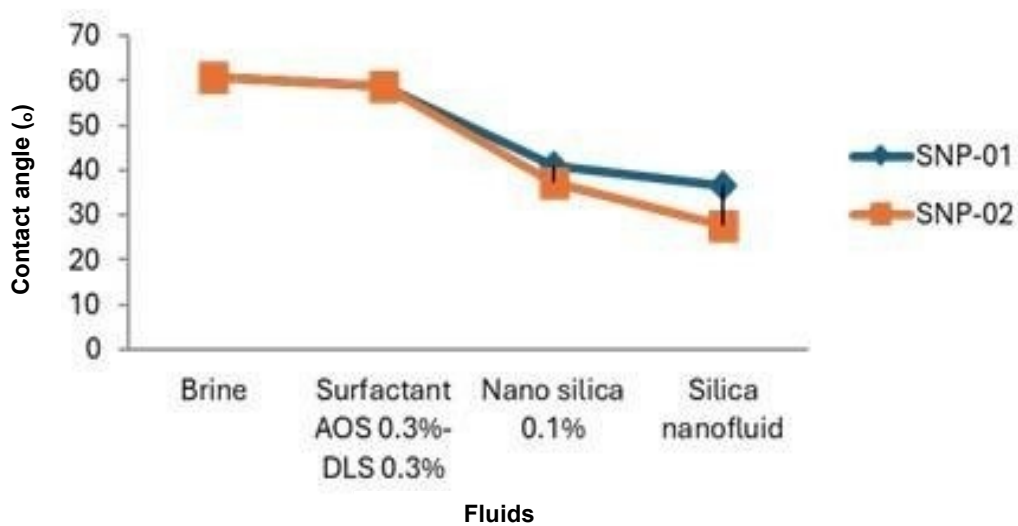


Figure 5. Effect of fluid solution type on contact angle.

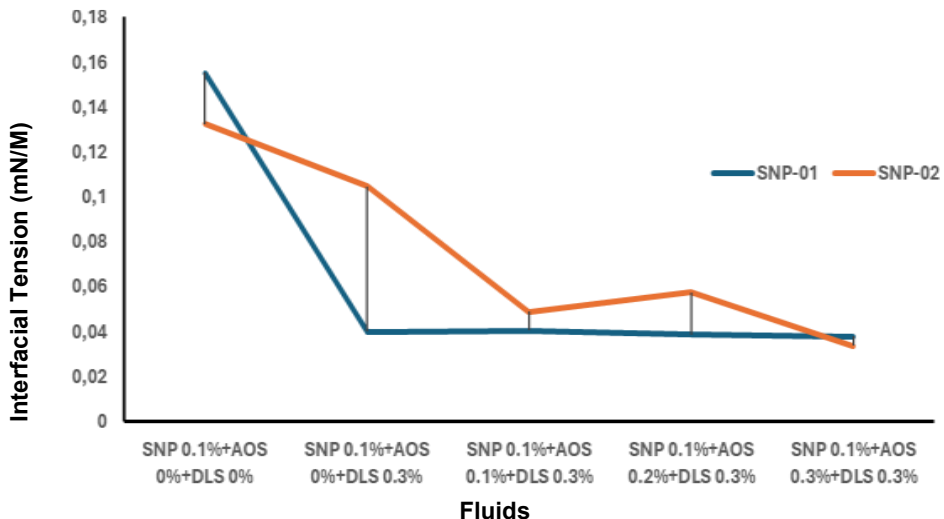


Figure 6. Effect of fluid solution type on IFT, illustrating the reduction of IFT due to the presence of anionic surfactant in silica nanofluid system.

nanosilica plays a significant role in lowering IFT and enhancing thermal stability. Other studies have reported that surfactant -based silica nanofluid formulations can effectively improve oil recovery compared to water floods, while also significantly reducing injection pressure compared to pure surfactant flooding. This work laid the foundation for the application of Ultralow IFT Nanofluid flooding technology in reservoirs with very low permeability (Xu et al., 2018).

Injectivity test

Injectivity tests were conducted to evaluate the effect of nanofluid injection with different nanosilica diameters on rock permeability and to assess the ability of nanofluids to flow through the core. This analysis is essential because the active nanosilica material in the nanofluid formulation has the potential to clog pore channels, leading to plugging. The results of the injectivity analysis indicate that the SNP01 and SNP02 nanofluid solutions exhibited high residual resistance factor (RRF) and resistance factor (RF) values above 1.0, which suggests the occurrence of core blockage (Table 7).

This plugging is attributed to the obstruction of rock pores by the silica nanofluid. Notably, the RRF value for SNP02 was lower than that for SNP01. Furthermore, delta-pressure data show that an increase in injection rate corresponds to a rise in pressure. The delta pressure observed during

SNP02 injection was lower than that during SNP01 injection (Table 8), indicating that the diameter of the silica nanoparticles significantly influences the injectivity and pressure behavior of the nanofluid.

Table 7. Injectivity test result

| Data | Rate (cc/min) | Nanofluids | |
|----------------------------------|---------------|------------|-------|
| | | SNP01 | SNP02 |
| | 0.3 | 3.2 | 2.26 |
| Resistance Factor (RF) | 0.5 | 3.88 | 2.67 |
| | 0.8 | 4.64 | 3.12 |
| | | | |
| Residual Resistance Factor (RRF) | 0.3 | 2.91 | 2.19 |
| | 0.5 | 3.13 | 2.3 |
| | 0.8 | 2.96 | 2.69 |

Table 8. Delta pressure injectivity test result

| Data | Rate (cc/min) | Delta pressure (psi) | |
|------------|---------------|----------------------|------------------|
| | | Nanofluid SNP-01 | Nanofluid SNP-02 |
| Pre-flush | 0.3 | 3.24 | 2.87 |
| | 0.5 | 7.73 | 5.91 |
| | 0.8 | 10.83 | 7.7 |
| Nano Flood | 0.3 | 10.38 | 6.48 |
| | 0.5 | 30.01 | 15.79 |
| | 0.8 | 50.23 | 24.02 |
| Post-flush | 0.3 | 9.43 | 6.8 |
| | 0.5 | 24.2 | 13.59 |
| | 0.8 | 32.03 | 20.71 |

Core flooding silica nanofluid

The core flood analysis using SNP-01 nanosilica, conducted with variations in pure surfactant fluid and 0.1% nanofluid, in a core measuring 1.5 inches in diameter and 2 inches in length, demonstrated a porosity of approximately 0.2 and a permeability of about 300 mD (Table 9). The results indicate that the incorporation of nanosilica positively impacts the incremental recovery factor (RF), increasing the original oil in place (OOIP) by 8.5%. Furthermore, the use of 0.1% nanofluids (comprising 0.1% nano-silica and AOS-DLS at 0.3%-0.3%) yielded even better results, with incremental RF reaching 9.7% OOIP and a total RF of 56.6% OOIP (Figure 6). This demonstrates that the addition of 0.1% SNP-01 nano-silica significantly enhances the oil recovery factor compared to using pure surfactants alone. In this case, the presence of SNPs in the nanofluid reduces rock wettability, thereby contributing to the incremental RF.

Figure 7 clearly shows that the addition of nano-silica significantly reduces the fluid volume required for oil recovery, as reflected by the injected pore volume (PV). Specifically, the incorporation of 0.1% nanosilica reduces the required volume of pure surfactant solution from 1 PV to 0.6 PV. In a subsequent core flooding experiment using SNP 02 nano-silica, conducted under the same experimental conditions as SNP 01, an enhanced oil recovery performance was observed. The nanofluid formulation containing 0.1% SNP 02, together with surfactants, resulted in an incremental oil recovery of 12.1% OOIP and a total recovery factor of 61% OOIP. These results indicate that SNP 02 demonstrates superior efficiency in enhancing oil recovery compared to SNP 01, as summarized in Table 10 and Figure 8).

Thus, it can be concluded that smaller silica nanoparticle diameters have a greater potential to enhance oil recovery. The findings of this study are consistent with those reported by Hendraningrat,

Table 9. Flooding nanofluid SNP 01

| Parameter | Fluid | |
|-------------------------------|---------------------------------|------------------------|
| | Surfactant AOS 0.3%-DLS 0.3% | Nano Fluid (SNP 01) |
| Core dimensions | | |
| Diameter (inc) | 1.5 | 1.5 |
| Long (inc) | 2 | 2 |
| Properties core | | |
| Pore volume (cc) | 11.9 | 11.6 |
| Porosity (%) | 20 | 20 |
| Permeabilty (mD) | 266 | 352 |
| OOIP in core (Soi) | | |
| Oil saturation (cc) | 6.7 | 6.4 |
| Oil saturation (%) | 56.2 | 55.1 |
| RF water flooding | | |
| Oil recovery (cc) | 3.1 | 3 |
| OOIP (%) | 45.5 | 46.9 |
| RF Chemical/ nano flooding | | |
| Oil recovery (cc) | 0.57 | 0.62 |
| OOIP (%) | 8.5 | 9.69 |
| RF Post Flush | | |
| Oil recovery (cc) | 0 | 0 |
| OOIP (%) | 0 | 0 |
| Total RF | | |
| Oil recovery (cc) | 3.7 | 3.6 |
| OOIP (%) | 54 | 56.6 |

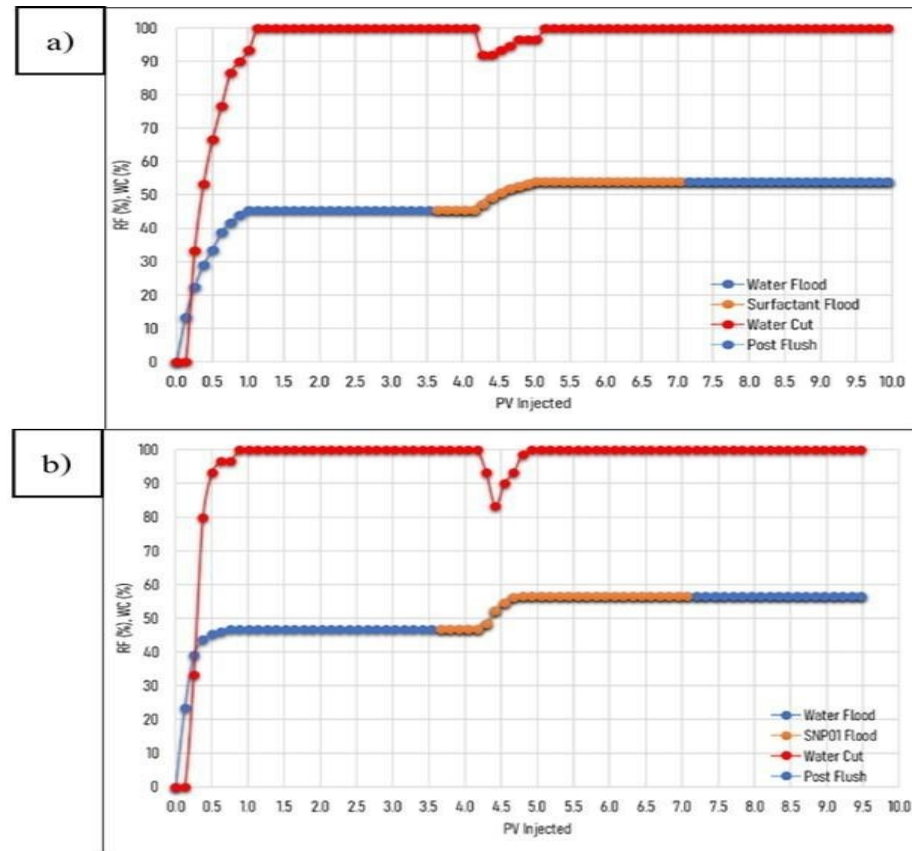


Figure 7. Results of core flooding experiments of SNP 01 nanofluids , a) surfactants flooding, b) nanofluid flooding, illustrating the effect of silica nanoparticles on EOR in sandstone cores.

Table 10. Core flooding nanofluid SNP 02

| Parameter | Fluid | |
|-------------------------------|---------------------------------|------------------------|
| | Surfactant AOS 0.3%-DLS 0.3% | Nano Fluid (SNP 02) |
| Core dimensions | | |
| Diameter (inc) | 1.5 | 1.5 |
| Long (inc) | 2 | 2 |
| Properties core | | |
| Pore volume (cc) | 11.9 | 12.1 |
| Porosity (%) | 20 | 20 |
| Permeability (mD) | 266 | 289 |
| OOIP in core (Soi) | | |
| Oil saturation (cc) | 6.7 | 6.75 |
| Oil saturation (%) | 56.2 | 55.9 |
| RF water flooding | | |
| Oil recovery (cc) | 3.1 | 3.3 |
| OOIP (%) | 45.5 | 46.9 |
| RF Chemical/ nano flooding | | |
| Oil recovery (cc) | 0.57 | 0.82 |
| OOIP (%) | 8.5 | 12.1 |
| RF Post Flush | | |
| Oil recovery (cc) | 0 | 0 |
| OOIP (%) | 0 | 0 |
| Total RF | | |
| Oil recovery (cc) | 3.7 | 4.1 |
| OOIP (%) | 54 | 61 |

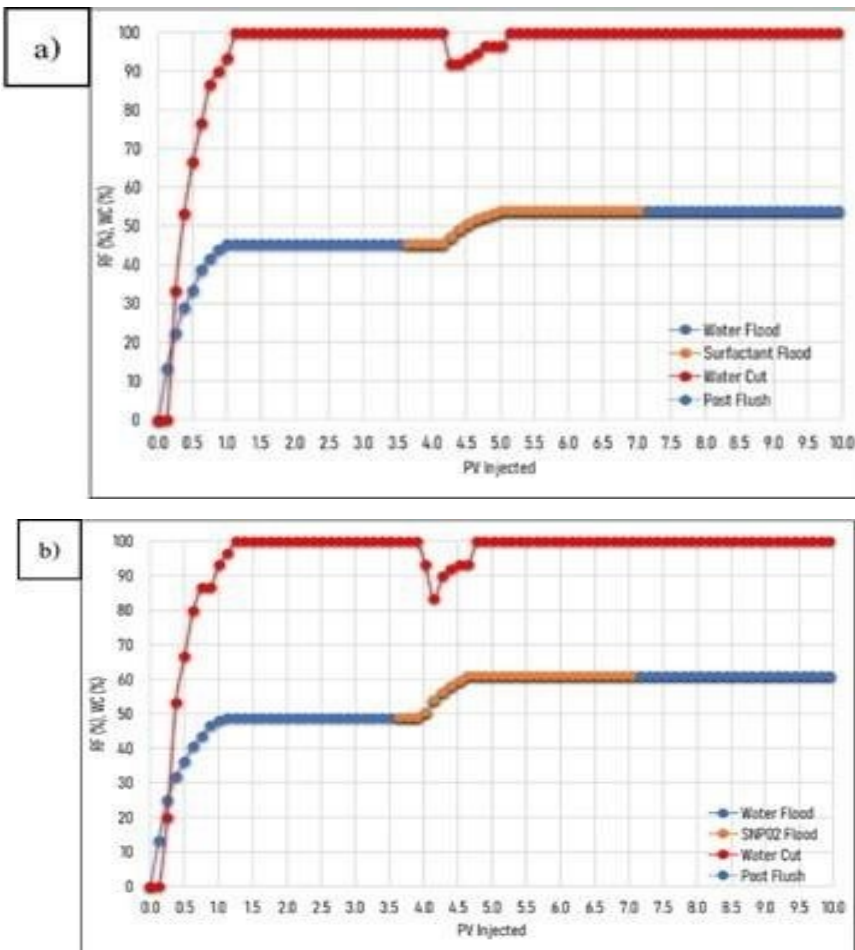


Figure 8. Results of core flooding experiments of SNP 02 nanofluids, a) AOS 0.3% -DLS 0.3% surfactant flooding, b) silica nanofluid flooding demonstrating EOR performance in sandstone cores..

who showed that oil recovery obtained using 7 nm silica nanoparticles was higher than that achieved with larger particles of 16 nm, 40 nm in diameter (Hendraningrat et al. 2013).

The higher RF obtained with SNP 02 nano-silica compared to SNP 01 is primarily due to its smaller particle diameter (3 nm), which enables improved mobility and deeper penetration into porous media. In addition, the lower contact angle achieved with SNP-02 contributes to more effective oil displacement, leading to higher recovery rates. Furthermore, the ability of SNP 02 to reduce the required injected pore volume (PV) highlights its effectiveness in minimizing the amount of chemicals needed during the core flooding process. These observations are consistent with the results obtained using SNP 01, further confirming the superior performance and efficiency of smaller-sized silica nanoparticles for EOR applications.

Morphological analysis of rocks by SEM

SEM analysis indicates that the application of nanofluids and surfactant is effective in reducing the concentration of impurity grains within the core rock, thereby improving pore accessibility (Figure 9). Prior to core flooding (Figure 9a), the rock surface exhibited particles of varying sizes and shapes, with a relatively rough texture and the presence of numerous impurities, such as clay minerals, which occupied and partially blocked the pore spaces. In contrast, the post flooding SEM images (Figure 9b and 9c), reveal noticeable morphological changes. The rock particles appear more open, indicating enhanced pore connectivity.

The results of this study show that the addition of AOS-DLS surfactant plays a crucial role in enhancing the thermal stability of nanofluids and reducing IFT. Meanwhile, the incorporating of smaller diameter silica nanoparticles contributes to

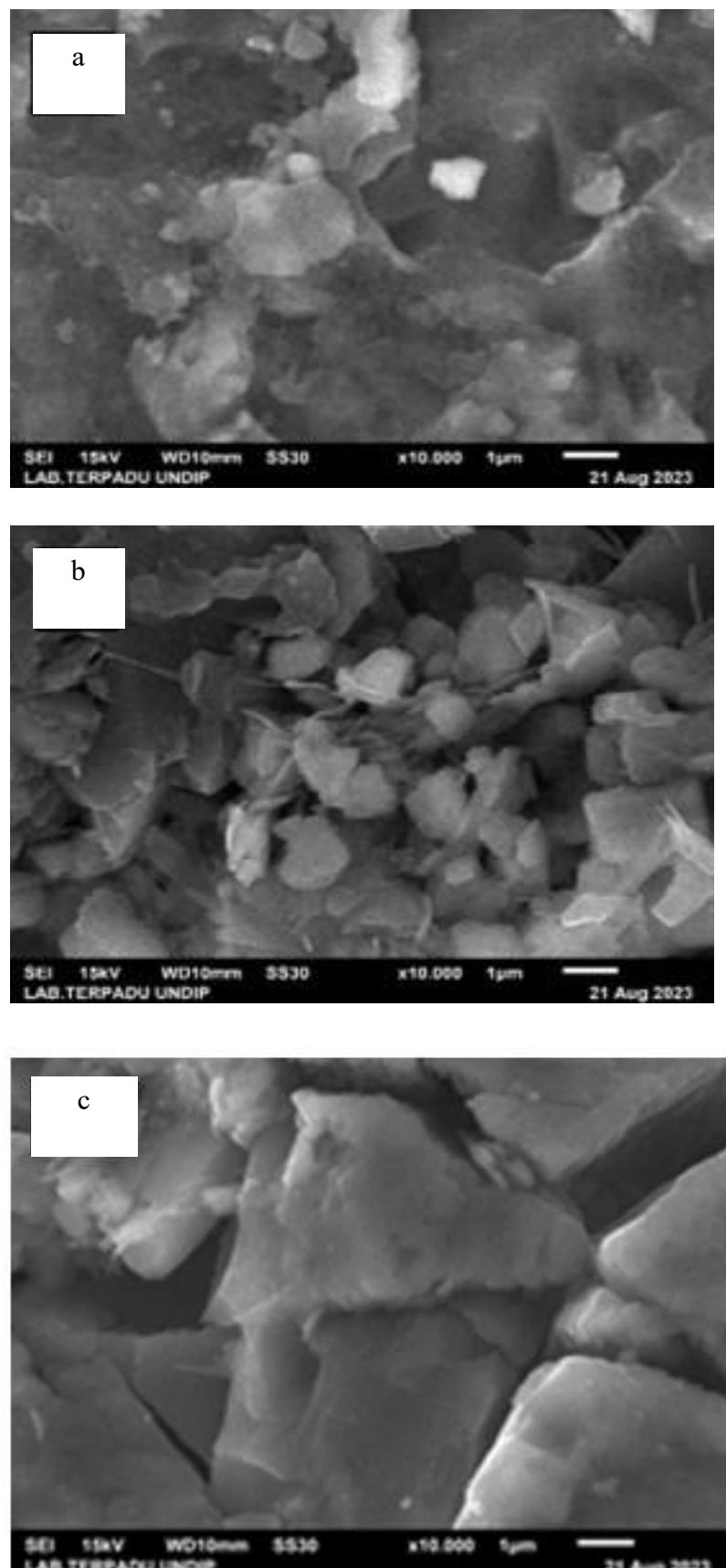


Figure 9. Result SEM analyst, a) before core flooding, b) after nanofluid core flooding, c) after surfactant flooding

wettability alteration, reduction of RF, RRF, and pressure drop, while simultaneously increasing oil recovery. The synergistic interaction between silica nanoparticles and anionic AOS-DLS surfactants is therefore essential for the development of optimized nanofluids suitable for EOR applications.

CONCLUSION

This study demonstrates that nano-silica stabilized with AOS-DLS surfactant at a concentration of 0.3% w/v exhibits excellent thermal stability, maintaining its properties within a temperature range of 60 to 80°C for over up to three months without producing deposits. An increase in nano-silica concentration leads to a reduction in the contact angle of the nanofluid, while its addition to the surfactant nanofluid does not significantly affect the IFT value. The findings highlight that the effectiveness of silica nanofluids in EOR is influenced by reductions in both contact angle and IFT values, which contribute to improved oil displacement. Furthermore, coreflood tests conducted on the upper gray Berea core using 0.1% SNP 02 nanofluid achieved the highest recovery factor of 12.1% of the OOIP, resulting in a total recovery factor of 61% of the OOIP. These results underscore the potential of silica nanofluids as a promising EOR agent in the field. However, this study was limited to the type of crude oil, rock porosity, and rock type used. Future research examining variations in crude oil types, rock porosities, and rock formations would be valuable for identifying optimal conditions for the field-scale application of silica nanofluids in EOR.

ACKNOWLEDGEMENT

We want to acknowledge the support from Diponegoro University and PT. Pertamina for this research. No. 4150282666.

GLOSSARY OF TERMS

| Symbol | Definition | Unit |
|-------------|--|------|
| IFT | Interfacial tension | mN/m |
| PV | Pore volume | cm |
| API Gravity | American Petroleum Institute gravity | |
| ASTM | American Society for Testing and Materials | |
| Si-OH | Silanol group | |
| Si-O | Siloxane group | |
| Soi | Initial oil saturation | |

REFERENCES

Abraham, D., Orodu, O., Efeovbokhan, V., Okoro, E., Ojo, T., & Keshinro, L. (2020). Experimental Studies on the Performance of Bio Based and Industrial Surfactants in Enhanced Oil Recovery. Paper presented at the SPE Nigeria Annual International Conference and Exhibition. doi: <https://doi.org/10.2118/203759-MS>.

Ahmed, A., Saaid, I. M., Ahmed, A. A., Pilus, R. M., & Baig, M. K. (2020). Evaluating the potential of surface-modified silica nanoparticles using internal olefin sulfonate for enhanced oil recovery. *Petroleum Science*, 17 (3), 722-733. doi:<https://10.1007/s12182-019-00404-1>.

Al-Shargabi, M., Davoodi, S., Wood, D. A., Al-Musai, A., Rukavishnikov, V. S., & Minaev, K. M. (2022). Nanoparticle applications as beneficial oil and gas drilling fluid additives: A review. *Journal of Molecular Liquids*, 352, 118725. doi:<https://doi.org/10.1016/j.molliq.2022.118725>.

Alsaba, M. T., Al Dushaishi, M. F., & Abbas, A. K. (2020). A comprehensive review of nanoparticles applications in the oil and gas industry. *Journal of Petroleum Exploration and Production Technology*, 10(4), 1389-1399.

doi:<https://doi.org/10.1007/s13202-019-00825-z> Behera, U. S., Poddar, S., Deshmukh, M. P., Sangwai, J. S., & Byun, H.-S. (2024). Comprehensive Review on the Role of Nanoparticles and Nanofluids in Chemical Enhanced Oil Recovery: Interfacial Phenomenon, Compatibility, Scalability, and Economic Viability. *Energy & Fuels*, 38(15), 13760-13795. doi:<https://doi.org/10.1021/acs.energyfuels.4c02248>.

Bila, A., & Torsæter, O. (2021). Experimental Investigation of Polymer-Coated Silica Nanoparticles for EOR under Harsh Reservoir Conditions of High Temperature and Salinity. *Nanomaterials*, 11(3), 765. doi:<https://doi.org/10.3390/nano11030765>.

Bratovic, A. (2023). Application of Nanofluids and Nanocomposites for Enhanced Oil Recovery. *Journal of Material Science and Technology*, 9 (1), 7-15.

Davoodi, S., Al-Shargabi, M., Wood, D. A., Rukavishnikov, V. S., & Minaev, K. M. (2022). Experimental and field applications of nanotechnology for enhanced oil recovery purposes: A review.

DN, A. A. P., & Szafdarian, R. A. J. L. p. m. d. g. b. (2023). Perbandingan Penggunaan Nano Silika dan Nano Abu Batubara pada Uji Kestabilan Busa untuk Injeksi CO₂. 57(2), 29-39. doi:<https://doi.org/10.29017/LPMGB.57.2.1577>.

Dong, P., Puerto, M., Ma, K., Mateen, K., Ren, G., Bourdarot, G., . . . Hirasaki, G. (2018). Ultralow-interfacial-tension foam injection strategy investigation in high temperature ultra-high salinity fractured carbonate reservoirs. Paper presented at the SPE Improved Oil Recovery Conference? doi: <https://doi.org/10.2118/190259-MS>.

Dordzie, G., & Dejam, M. (2021). Enhanced oil recovery from fractured carbonate reservoirs using nanoparticles with low salinity water and surfactant: A review on experimental and simulation studies. *Advances in Colloid and Interface Science*, 293, 102449. doi:<https://doi.org/10.1016/j.cis.2021.102449>

Fathaddin, M. T., Prapansya, O. R., Rakhmanto, P. A., Mardiana, D. A., Septianingrum, W. A., Irawan, S., Gas. (2025). The Effect of TiO₂ Nanoparticles on The Performance of Kappaphycus Alvarezii Biopolymer for Enhanced Oil Recovery. 48(3), 327-339. doi:<https://doi.org/10.29017/scog.v48i3.1909>.

Franco, C. A., Franco, C. A., Zabala, R. D., Bahamón, I., Forero, Á., & Cortés, F. B. (2021). Field Applications of Nanotechnology in the Oil and Gas Industry: Recent Advances and Perspectives. *Energy & Fuels*, 35(23), 19266-19287. doi:<https://doi.org/10.1021/acs.energyfuels.1c02614>

Fu, L., Gu, F., Liao, K., Wen, X., Jiang, L., Li, X., Shao, M. (2022). Molecular dynamics simulation of enhancing surfactant flooding performance by using SiO₂ nanoparticles. *Journal of Molecular Liquids*, 367, 120404. doi:<https://doi.org/10.1016/j.molliq.2022.120404>.

Hadia, N. J., Ng, Y. H., Stubbs, L. P., & Torsæter, O. (2021). High Salinity and High Temperature Stable Colloidal Silica Nanoparticles with Wettability Alteration Ability for EOR Applications. *Nanomaterials*, 11(3), 707.

Hendraningrat, L., Li, S., & Torsæter, O. (2013). Effect of some parameters influencing enhanced oil recovery process using silica nanoparticles: an experimental investigation. Paper presented at the SPE Reservoir Characterisation and Simulation Conference and Exhibition. doi: <https://doi.org/10.2118/165955-MS>.

Hu, T., Zhang, J., Xia, J., Li, X., Tao, P., & Deng, T. (2023). A Review on Recent Progress in Preparation of Medium-Temperature Solar-Thermal Nanofluids with Stable Dispersion. *Nanomaterials*, 13(8), 1399. doi:<https://doi.org/10.3390/nano13081399>.

Kumar, G., Behera, U. S., Mani, E., & Sangwai, J. S. (2022). Engineering the Wettability Alteration of Sandstone Using Surfactant-Assisted Functional Silica Nanofluids in Low-Salinity Seawater for Enhanced Oil Recovery. *ACS Engineering Au*, 2(5), 421-435.

Li, S., Ng, Y. H., Lau, H. C., Torsæter, O., & Stubbs, L. P. J. N. (2020). Experimental investigation of stability of silica nanoparticles at reservoir conditions for enhanced oil recovery applications. 10(8), 1522.

Malozymov, B. V., Martyushev, N. V., Kukartsev, V. V., Tynchenko, V. S., Bukhtoyarov, V. V., Wu, X., . . . Kukartsev, V. A. (2023). Overview of Methods for Enhanced Oil Recovery from Conventional and Unconventional Reservoirs. *Energies*, 16 (13), 4907.

Mmbuji, A. O., Cao, R., Li, Y., Xu, X., & Ricky, E. X. (2023). Nanoparticle-Assisted Surfactant/Polymer Formulations for Enhanced Oil Recovery in Sandstone Reservoirs: From Molecular Interaction to Field Application. *Energy & Fuels*, 37(22), 17094-17112. doi:<https://doi.org/10.1021/acs.energyfuels.3c02742>

Panchal, H., Patel, H., Patel, J., & Shah, M. (2021). A systematic review on nanotechnology in enhanced oil recovery. *Petroleum Research*, 6 (3), 204-212. doi:<https://doi.org/10.1016/j.ptlrs.2021.03.003>.

Paramastya, A., Chandra, S., Daton, W. N., Rachmat, S. J. S. C. O., & Gas. (2019). Nano-Surfactant Huff And Puff Optimatization In Marginal X Field Using Commercial Simulator . 42(2), 51-57.<https://doi.org/10.29017/SCOG.42.2.375>

Philip, J. (2023). Magnetic nanofluids (Ferrofluids): Recent advances, applications, challenges, and future directions. *Advances in Colloid and Interface Science*, 311, 102810. doi:<https://doi.org/10.1016/j.cis.2022.102810>

Sharma, P., Guha, A., & Das, S. (2024). Impact and challenges of nanotechnology in enhanced oil recovery. *Materials Today: Proceedings*, 99, 126-131.

doi:<https://doi.org/10.1016/j.matpr.2023.05.655>

Shayan Nasr, M., Esmaeilnezhad, E., & Choi, H. J. (2021). Effect of silicon-based nanoparticles on enhanced oil recovery: Review. *Journal of the Taiwan Institute of Chemical Engineers*, 122, 241-259. doi:<https://doi.org/10.1016/j.ptlrs.2021.04.047>

Sircar, A., Rayavarapu, K., Bist, N., Yadav, K., & Singh, S. (2022). Applications of nanoparticles in enhanced oil recovery. *Petroleum Research*, 7(1), 77-90. doi:<https://doi.org/10.1016/j.ptlrs.2021.08.004>

Xu, D., Bai, B., Meng, Z., Zhou, Q., Li, Z., Lu, Y., Kang, W. (2018). A novel ultra-low interfacial tension nanofluid for enhanced oil recovery in super-low permeability reservoirs. Paper presented at the SPE asia pacific oil and Gas conference and exhibition. doi: <https://doi.org/10.2118/192113-MS>.